NANO LETTERS

Letter

pubs.acs.org/NanoLett

Panchromatic Photon-Harvesting by Hole-Conducting Materials in Inorganic−Organic Heterojunction Sensitized-Solar Cell through the Formation of Nanostructured Electron Channels

Jeong Ah Chang,[†] Sang Hyuk Im,[†] Yong Hui Lee,[†] Hi-jung Kim, Choong-Sun Lim, Jin Hyuk Heo, and Sang Il Seok*

Solar Energy Materials Research Group, Division of Advanced Materials, Korea Research Institute of Chemical Technology, 141 Gajeong-ro, Yuseong-gu, Daejeon 305-600, Korea

Supporting Information

ABSTRACT: Additional photon-harvesting by hole transporting materials in Sb_2S_3-sensitized solar cell is demonstrated through the formation of electron channels in the hole transporter such as P3HT (poly(3-hexylthiophene)) and PCPDTBT(poly(2,6-(4,4-bis-(2-ethylhexyl)-4*H*-cyclopenta[2,1-*b*;3,4-*b*′]dithiophene)-alt-4,7(2,1,3-benzothiadiazole)) that can act as both a hole conductor and light absorber. As a result, the short-circuit current density is improved with an increment in overall efficiency. These findings provide new insights into use of light-absorbing conjugated polymers as a hole conductor in the inorganic−organic heterojunction sensitized solar cells.

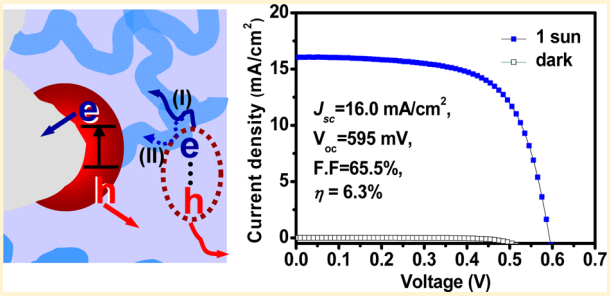

KEYWORDS: *Electron channel, Sb_2S_3, hole-conducting materials, inorganic−organic heterojunction, solar cells*

Inorganic-semiconductor-based extreme thin absorbers (ETAs) or sensitized solar cells have been considered as promising next generation solar cells whose performance could exceed conventional dye-sensitized solar cells (D-SSCs) since Grätzel et al.[1−3] developed highly efficient solar cells with a power conversion efficiency over 11% under 1 sun illumination. Metal chalcogenides in particular, such as CdS, CdSe, CdTe, PbS, PbSe, and Sb_2S_3, have been extensively studied as new light absorbers or sensitizers to replace conventional ruthenium/organic sensitizers in order to attain high-device performance because such inorganic metal chalcogenides have unique properties such as a higher extinction coefficient than ruthenium/organic dyes, easy charge separation by a large dipole moment, convenient bandgap tuning by the quantum confinement effect, multiple exciton generation, and good stability.[4−12]

Among the metal chalcogenides, Sb_2S_3 seems to be a very attractive material as a light absorber because it has a strong absorption coefficient (1.8×10^5 cm^{-1} in the visible region) and an appropriate bandgap (E_g = 1.7 eV).[13−16] Crystalline Sb_2S_3 (stibnite) has been deposited on mesoporous TiO_2 (mp-TiO_2) by chemical bath deposition (CBD).[14−16] Itzhaik et al.[17] have reported Sb_2S_3/CuSCN ETA solar cells with a power conversion efficiency of 3.4% under 1 sun irradiation, and Moon et al.[18] have also reported a power conversion efficiency of 3.1% for solid-state Sb_2S_3-sensitized solar cells comprising mp-TiO_2/Sb_2S_3/spiro-MeOTAD (2,2′,7,7′-tetrakis(*N*,*N*-di-*p*-methoxyphenylamine)-9,9′-spirobi-fluorene). Recently, we reported a high efficient inorganic/organic heterojunction solid-state Sb_2S_3-sensitized solar cell with conjugated polymers as hole-transporting materials (HTMs) like P3HT (poly(3-hexylthiophene)) and PCPDTBT (poly(2,6-(4,4-bis-(2-ethylhexyl)-4*H*-cyclopenta[2,1-*b*;3,4-*b*′]dithiophene)-alt-4,7(2,1,3-benzothiadiazole))[19,20] and a liquid-type Sb_2S_3-sensitized solar cell working in a cobalt redox electrolyte.[21] Unlike Sb_2S_3-based ETAs and sensitized solar cells using wide bandgap hole-transporting materials without significant absorption of visible light,[17,18] the Sb_2S_3-sensitized heterojunction solar cell revealed a lower external quantum efficiency (EQE) in the specific wavelength range of 450−650 nm because the P3HT hole-conducting polymer coabsorbs light in this wavelength range and the charge carriers generated by P3HT are not completely transferred to either the photoanode or Au counter electrode.[19,21] Therefore, we cannot avoid EQE loss in the absorption region caused by the P3HT hole-conducting polymer as long as the generated charge carriers in P3HT are not extracted efficiently. How then can we avoid EQE loss from the coabsorbed light by P3HT in Sb_2S_3-sensitized heterojunction solar cells? Intuitively, the answer will be to find new hole-conductors having a nonoverlapping absorption band with Sb_2S_3, such as wide or low bandgap materials, or to find a way to recover the EQE lost by P3HT coabsorption via extraction of the generated electron−hole pairs in P3HT to the photoanode and photocathode. Herein, we propose an efficient

Received: December 1, 2011
Revised: February 19, 2012

   dx.doi.org/10.1021/nl204224v | *Nano Lett.* XXXX, XXX, XXX−XXX

way to recover the EQE lost by P3HT coabsorption in Sb_2S_3-sensitized heterojunction solar cells through the latter option. Furthermore, we demonstrate panchromatic light harvesting in TiO_2/Sb_2S_3/PCPDTBT(PCBM) devices by the same approaches.

In our previous study, we found that the generated electron−hole pairs in Sb_2S_3 could be efficiently transported into the TiO_2 electron conductor and P3HT hole-conducting layer; at the same time, the generated charge carriers in P3HT could be partially transported into TiO_2 and Sb_2S_3 for electrons and the Au electrode for holes.[19] Here, we conceive that if we can locate the electron channels bridging TiO_2 and bulk P3HT then we can recover the EQE lost by absorption of P3HT as long as the electron channels satisfy the following conditions: (i) the generated electron−hole pairs in P3HT can be efficiently separated at the P3HT/electron channel interface; (ii) the separated electrons are effectively injected into the electron channel and are safely delivered to either TiO_2 or Sb_2S_3; (iii) the delivered electrons through the electron channel should be more efficiently injected to either TiO_2 or Sb_2S_3 than the electron injection from P3HT to either TiO_2 or Sb_2S_3; and (iv) the recombination at the newly formed Sb_2S_3/electron channel interface should be insignificant (in other words, the lowest unoccupied molecular orbital (LUMO) energy level of the electron channel should be higher than the conduction band energy level of Sb_2S_3 to prevent reverse-directed electron transfer from Sb_2S_3 to the electron channel). On the basis of this concept, we chose a PCBM ([6,6]-phenyl-C_{61}-butyric acid methyl ester) as a model electron channel because PCBM is known as one of best electron acceptors compatible with the P3HT electron donor in bulk heterojunction (BHJ) solar cells, and the LUMO energy level is located at ca. −3.7 eV.[22] Figure 1 shows a schematic illustration of the device structure and its

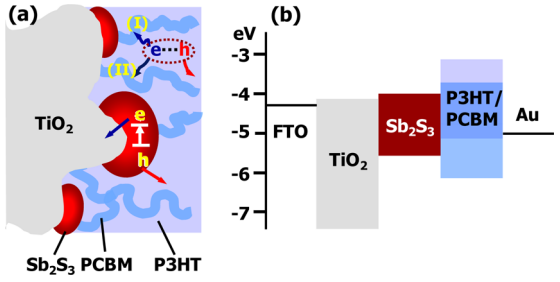

Figure 1. (a) Schematic illustration of the device structure and (b) its energy band diagram.

energy band diagram. The energy positions of the TiO_2/Sb_2S_3/P3HT and PCBM was depicted from reported values.[19−24]

It appears to be difficult to selectively locate the electron channels on an individual TiO_2 or Sb_2S_3 surface; consequently, the PCBM electron channels might be nonselectively formed as shown in Figure 1a. Thus, we need to determine which electron channel, either channel (I) or (II) in Figures 1a and 2a, is more desirable to efficiently deliver the generated charge carriers in P3HT. To compare the effect of the constructed electron channels (I) and (II), we designed model systems that formed channel (I) or (II) selectively. For a model device with electron channel (I) only, we deposited a P3HT (15 mg/1 mL of 1,2 dichlorobenzene) and a P3HT/PCBM (1:0.7 wt/wt: 15 mg/10.5 mg in 1 mL of 1,2 dichlorobenzene) film on a dense TiO_2 blocking layer (bl-TiO_2) of FTO (fluorine-doped SnO_2) substrate by spin coating. On the other hand, for the model device with electron channel (II) only we deposited the same P3HT and P3HT/PCBM film on a FTO/bl-TiO_2/Sb_2S_3 substrate in which the Sb_2S_3 is deposited on the FTO/bl-TiO_2 substrate by CBD. The scanning electron microscopy (SEM) cross-sectional image of the FTO/bl-TiO_2/Sb_2S_3 substrate in Figure 1b and Supporting Information Figure S1 confirms that the surface of the FTO/bl-TiO_2 substrate is fully covered by Sb_2S_3 thin film and, consequently, we can selectively form the electron channel (II).

Figure 2c shows the EQE spectra of the model devices for electron channels (I) and (II). The spectrum for the FTO/bl-TiO_2/P3HT (b-T/P) device without electron channel (I) shows that the generated electron−hole pairs in P3HT are not effectively transported to the bl-TiO_2 layer owing to an insufficient interface area at the n−p junction and inefficient charge transport. Even if we replace this bilayer-type (b-T/P) device with an inorganic−organic bulk heterojunction (I-O BHJ) type (mp-TiO_2/P3HT: acceptor/donor) cell, the performance of the I-O BHJ cell is only slightly better than that of the bilayer-type cell. This implies that the poor device performance is mainly caused by inefficient charge transport between bl-TiO_2 (or mp-TiO_2) and P3HT and not by insufficient interface area of the n−p junction. On the contrary, the FTO/bl-TiO_2/P3HT/PCBM (b-T/P-P) device with electron channel (I) shows greatly improved EQE values. This is not surprising because this device structure is similar to an inverted organic photovoltaic (OPV) cell. However, it should be noted that the newly formed PCBM electron channel bridging bl-TiO_2 and P3HT plays a critical role in transporting the generated charge carriers in P3HT into bl-TiO_2. It is well-known that the generated charge carriers in P3HT are efficiently separated at the P3HT/PCBM interface, and electrons are injected into PCBM; however, the charge transfer at bl-TiO_2/P3HT is not efficient under our device conditions. In addition, this shows that the separated electrons at the P3HT/PCBM interface are efficiently transported to the bl-TiO_2 layer via the PCBM electron channels. Therefore, PCBM is a good candidate for satisfying the previously mentioned conditions. On the other hand, the FTO/bl-TiO_2/Sb_2S_3/P3HT (b-T/S/P) device without electron channel (II) reveals better EQE values than the FTO/bl-TiO_2/Sb_2S_3/P3HT/PCBM (b-T/S/P-P) device with electron channel (II), as shown in Figure 2c. The deterioration of the EQE values of the b-T/S/P-P model device compared to the b-T/S/P model device might be attributed to the reduced effective contact interface between Sb_2S_3 and P3HT or to the inefficient charge transfer between Sb_2S_3 and PCBM electron channel (II) having electrons injected from P3HT coabsorber. From the band energy diagram in Figure 1b, the charge transfer at the Sb_2S_3/PCBM interface might be favorable, and, consequently, the reduced effective interface of Sb_2S_3/P3HT will mainly deteriorate the EQE values because generated holes cannot be effectively transferred to P3HT by the reduced contact area with Sb_2S_3. From the above model experiments, it is expected that we can transport, more efficiently, the generated electron−hole pairs in P3HT through the PCBM electron channel (I), and as a result the EQE lost by absorption of P3HT will be recovered by the construction of the PCBM electron channel. The corresponding current density−voltage (J−V) curves of the model devices match well with their EQE spectra, as shown in Figure 2d.

With the conviction that the PCBM electron channel can recover the EQE lost by coabsorption of P3HT, we fabricated the FTO/mp-TiO_2/Sb_2S_3/P3HT (T/S/P) and FTO/mp-

dx.doi.org/10.1021/nl204224v | Nano Lett. XXXX, XXX, XXX−XXX

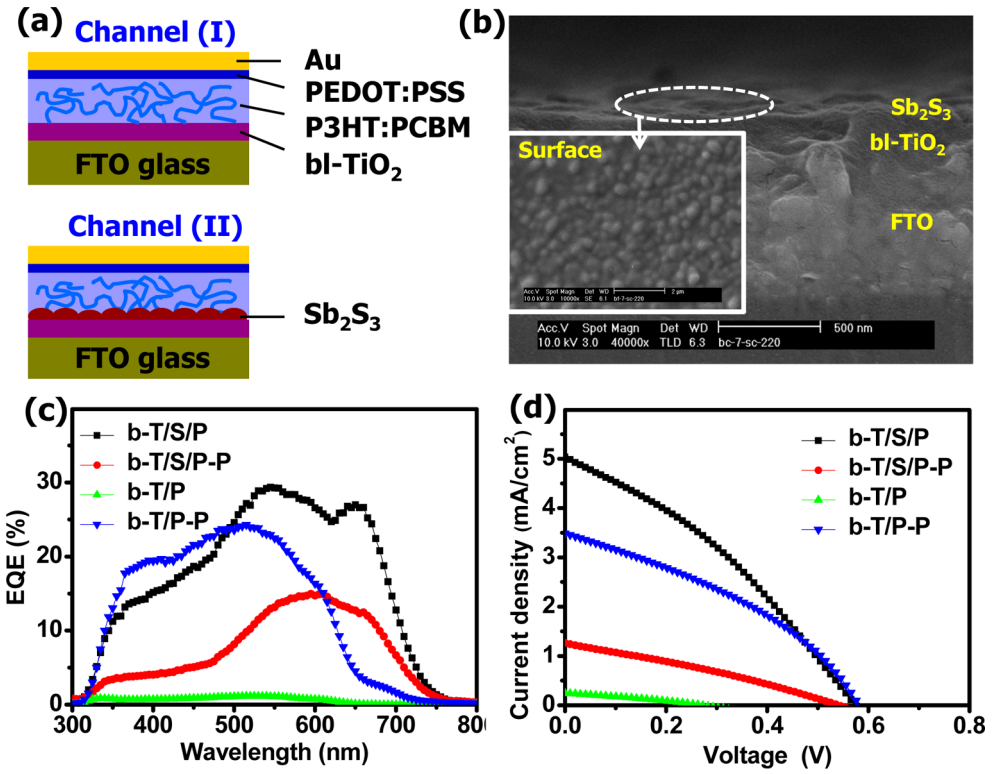

Figure 2. (a) Schematic device structure of the model experiments for channels (I) and (II); (b) cross-sectional SEM image of Sb_2S_3 film deposited on bl-TiO_2/FTO; (c) the EQE spectra of the model devices and (d) their *I*–*V* curves. The following abbreviations are used in the figure: b-T = bl-TiO_2, S = Sb_2S_3, P = P3HT, and P-P = P3HT/PCBM.

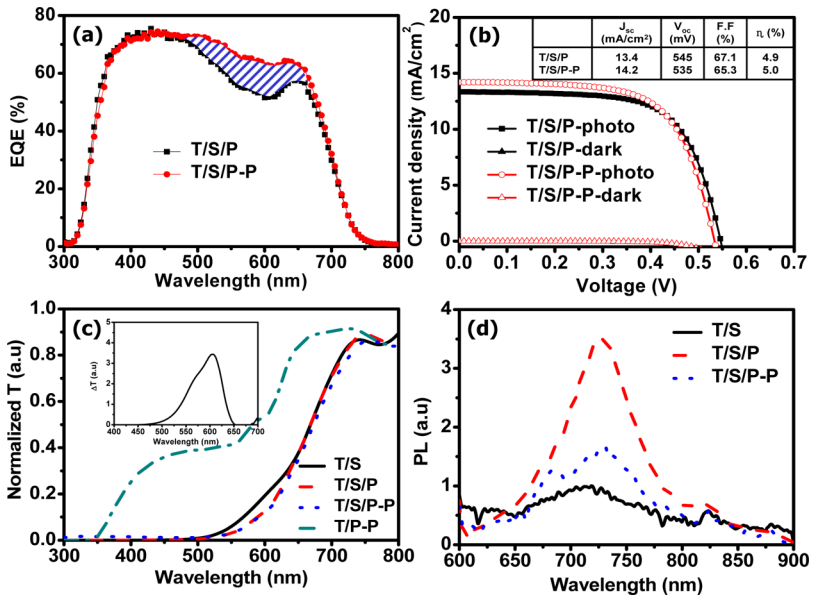

Figure 3. (a) EQE spectra: the region marked by the blue lines is the EQE difference between the T/S/P-P and T/S/P samples. (b) *J*–*V* curves at 100 mW/cm^2 light illumination (photo) and no illumination (dark). (c) Transmission spectra: the inset shows the transmission difference between the T/S/P(-P) and T/S/P samples. (d) PL spectra. The following abbreviations are used in the figure: T = mp-TiO_2, S = Sb_2S_3, P = P3HT, and P-P = P3HT/PCBM.

TiO_2/Sb_2S_3/P3HT/PCBM (T/S/P-P) devices. Figure 3a shows the EQE spectra of the T/S/P and T/S/P-P devices and clearly confirms that the PCBM electron channel substantially recovers the EQE loss caused by absorption of P3HT (additional EQE spectra of different samples are shown in Supporting Information Figure S2, confirming that the newly constructed PCBM electron channel could additionally extract the generated charge carriers in P3HT to mp-TiO_2). Supporting Information Figure S3 shows the EQE spectra of the T/S/P and T/S/P-P devices at different CBD times (0, 1, and 1.5 h). As the CBD time increases, the amount of Sb_2S_3 deposited on mp-TiO_2 increases. These EQE spectra clearly indicate that the T/S/P-P samples with the PCBM electron channel always reveal higher EQE values than the T/S/P

dx.doi.org/10.1021/nl204224v | *Nano Lett.* XXXX, XXX, XXX–XXX

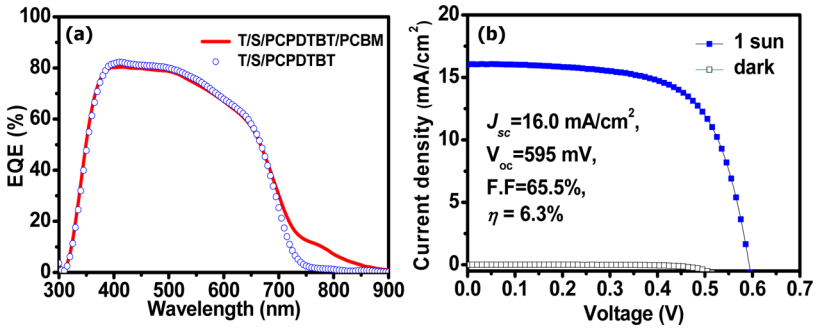

Figure 4. (a) EQE spectra for devices fabricated without and with PCBM in PCPDTBT and (b) $J-V$ curves of mp-TiO_2/Sb_2S_3/PCPDTBT-PCBM device.

samples without an electron channel. This result agrees well with the model experiments because the newly constructed PCBM electron channel bridging P3HT and mp-TiO_2 could more effectively transport the generated charge carriers in P3HT to mp-TiO_2 as a result of more efficient charge transfer in the PCBM/P3HT interface than the mp-TiO_2/P3HT interface. In the case of samples having a lower concentration of Sb_2S_3 for short CBD time periods (0 h, 1 h, and 1.5 h), the EQE values of samples with PCBM electron channels are higher than those without electron channels across the whole visible region because the unabsorbed light is coabsorbed by P3HT, and consequently the P3HT generates charge carriers that are transported through the PCBM electron channel. The gradual decrease of the EQE difference between the samples with electron channels and those without electron channels along with the CBD time period is attributed to the gradual increase of absorption by Sb_2S_3 deposited on mp-TiO_2. Accordingly, the Sb_2S_3 prepared by 2 h of CBD absorbs most of the light, and the light not absorbed by Sb_2S_3 is absorbed by P3HT. As expected from the EQE spectra, the short-circuit current density (J_{sc} = 14.2 mA/cm^2) of the T/S/P-P device is higher than the short-circuit current density (J_{sc} = 13.4 mA/cm^2) of the T/S/P device, as shown in Figure 3b. By integrating the difference between the EQE spectra (the region marked by the blue lines in Figure 3a), we can expect that a J_{sc} of 1.0 mA/cm^2 under an illumination of 100 mW/cm^2 can be generated. This agrees well with the J_{sc} difference (0.8 mA/cm^2) of the T/S/P-P and T/S/P devices. Accordingly, the overall power conversion efficiency of T/S/P-P (η = 5.0%) is improved more than that of T/S/P (η = 4.9%), although the fill factor of the T/S/P-P (65.3%) device is slightly lower than that of T/S/P (67.1%). Therefore, the improved overall power conversion efficiency was mainly attributed to the recovered EQE by the constructed PCBM electron channel bridging P3HT and mp-TiO_2, and the slight deterioration of the fill factor might be attributed to the reduced effective contacting interface between Sb_2S_3 and P3HT as a result of formation of PCBM electron channel (II).

To confirm that the major contribution to the device efficiency is the constructed PCBM electron channel, we compared the transmission spectra of each device, as shown in Figure 3c, because the EQE value is the product of the light-harvesting, charge injection, and charge collection efficiencies. An absorption by P3HT/PCBM in mp-TiO_2, as can be seen in the transmittance measured from T/P-P, at the shorter wavelength region below 550 nm is relatively low. This is ascribed by a low molar absorption coefficient of P3HT, compared to the Sb_2S_3.[24,25] This indicates P3HT/PCBM cannot effectively contribute to the light harvesting at the shorter wavelength region in mp-TiO_2/Sb_2S_3/P3HT(PCBM) devices. The identical transmission spectra for T/S/P and T/S/P-P mean that the light-harvesting efficiency of both cells is the same. Hence, the improved EQE value achieved by the constructed PCBM electron channel is attributed to the enhanced charge injection or charge collection efficiency. The different transmission spectra for T/S and T/S/P (or T/S/P-P), shown in the inset of Figure 3c, corresponds to the absorption by P3HT, and the absorption region agrees well with the EQE loss region in Figure 3a. In order to support that the charge carriers in P3HT generated by coabsorption could be more efficiently transported via the constructed PCBM electron channel, we checked the photoluminescence (PL) spectra of the T/S, T/S/P, and T/S/P-P devices under excitation by 530 nm wavelength light, as shown in Figure 3d. The depressed PL spectrum of the T/S/P-P sample compared to the T/S/P sample indicates that the generated charge carriers in P3HT are more efficiently separated in the T/S/P-P sample as a result of the constructed PCBM electron channel. This might be attributed to the fact that the generated charge carriers in P3HT are more efficiently separated at the P3HT/PCBM interface than at the P3HT/mp-TiO_2 interface. From the transmission, EQE, and PL spectra, we can conclude that the constructed PCBM electron channel could improve the charge injection and charge collection efficiencies.

Efficient charge collection through PCBM electron channel was successfully applied to the low band gap hole conducting polymer to harvest additional sunlight. For this purpose, we used PCPDTBT in the place of P3HT. Figure 4a confirms that the light absorbed by PCPDTBT/PCBM in a near-infrared region contributes to generate additional charges from the comparison of the EQE spectra for devices fabricated without and with PCBM in PCPDTBT. The use of the low band gap hole conducting polymer assisted by PCBM electron channel enables the J_{sc} of the cell to be reached 16 mA/cm^2 and 6.3% of power conversion efficiency (η) under air mass 1.5 global (AM1.5G) illumination with the intensity of 100 mW/cm^2, as shown in Figure 4b. To the best of our knowledge, this cell provides the highest values of overall conversion efficiency ever reported in the inorganic semiconductor-sensitized solid-state solar cells.

In summary, we could effectively overcome the filter effect caused by absorption of P3HT in the visible range through the formation of electron channels in a hole-conducting material. The newly constructed PCBM electron channel bridging mp-TiO_2 and P3HT could additionally transfer the generated charge carriers in P3HT to mp-TiO_2. From model experiments,

dx.doi.org/10.1021/nl204224v | Nano Lett. XXXX, XXX, XXX–XXX

we found that PCBM electron channel (I) bridging mp-TiO_2 and P3HT is more positive than electron channel (II) bridging Sb_2S_3 and P3HT because electron channel (II) might hinder the efficient hole extraction from Sb_2S_3 to P3HT as a result of a reduced effective interface between Sb_2S_3 and P3HT. Moreover, we could collect additional charge produced by PCPDTBT as low band gap hole conducting polymer that can absorb light in a near-infrared region. We believe that the present findings provide novel directions for achieving high-efficiency solid-state solar cells using hole-conducting materials.

■ ASSOCIATED CONTENT

Ⓢ Supporting Information

Details of experiments and additional supplementary figures. This material is available free of charge via the Internet at http://pubs.acs.org.

■ AUTHOR INFORMATION

Corresponding Author

*E-mail: seoksi@krict.re.kr.

Author Contributions

†These authors contributed equally to this work.

Notes

The authors declare no competing financial interest.

■ ACKNOWLEDGMENTS

This study was supported by the Global Research Laboratory (GRL) Program and the Global Frontier R&D Program on Center for Multiscale Energy System funded by the National Research Foundation under the Ministry of Education, Science and Technology of Korea and by a grant from the KRICT 2020 Program for Future Technology of the Korea Research Institute of Chemical Technology (KRICT), Republic of Korea.

■ REFERENCES

(1) O'Regan, B.; Grätzel, M. *Nature* **1991**, *353*, 737−740.

(2) Bessho, T.; Zakeeruddin, S. M.; Yeh, C. −Y.; Diau, E. W. -G.; Grätzel, M. *Angew. Chem., Int. Ed.* **2010**, *49*, 6646−6649.

(3) Chen, C.; Wang, M.; Li, J.; Pootrakulchote, N.; Alibabaei, L.; Ngocle, C.; Decoppet, J.-D.; Tsai, J. H.; Grätzel, C.; Wu, C.-G.; Zakeeruddin, S. M.; Grätzel, M. *ACS Nano* **2009**, *3*, 3103−3109.

(4) Lee, Y. H.; Im, S. H.; Rhee, J. H.; Lee, J. −H.; Seok, S. I. *ACS Appl. Mater. Interfaces* **2010**, *2*, 1648−1652.

(5) Lee, Y. H.; Im, S. H.; Lee, J. −H.; Seok, S. I. *Electrochim. Acta* **2011**, *56*, 2087−2091.

(6) Im, S. H.; Lee, Y. H.; Seok, S. I. *Electrochim. Acta* **2010**, *55*, 5665−5669.

(7) Im, S. H.; Lee, Y. H.; Seok, S. I.; Kim, S. W.; Kim, S. -W. *Langmuir* **2010**, *26*, 18576−18580.

(8) Lee, Y.-L.; Lo, Y.-S. *Adv. Funct. Mater.* **2009**, *19*, 604−609.

(9) Lee, H.; Wang, M.; Chen, P.; Gamelin, D. R.; Zakeeruddin, S. M.; Grätzel, M.; Nazeeruddin, Md. K. *Nano Lett.* **2009**, *9*, 4221−4227.

(10) Im, S. H.; Chang, J. A.; Kim, S. W.; Kim, S.-W.; Seok, S. I. *Org. Electron.* **2010**, *11*, 696−699.

(11) Nozik, A. J. *Chem. Phys. Lett.* **2008**, *457*, 3−11.

(12) Costi, R.; Saunders, A. E.; Banin, U. *Angew. Chem., Int. Ed.* **2010**, *49*, 4878−4897.

(13) Versavel, M. Y.; Haber, J. A. *Thin Solid Films* **2007**, *515*, 7171−7276.

(14) Messina, S.; Nair, M. T. S.; Nair, P. K. *Thin Solid Films* **2009**, *517*, 2503−2507.

(15) Nair, M. T. S.; Peña, Y.; Campos, J.; García, V. M.; Nair, P. K. *J. Electrochem. Soc.* **1998**, *145*, 2113−2120.

(16) Messina, S.; Nair, M. T. S.; Nair, P. K. *Thin Solid Films* **2007**, *515*, 5777−5782.

(17) Yafit, I.; Olivia, N.; Miles, P.; Gary, H. *J. Phys. Chem. C* **2009**, *113*, 4254−4256.

(18) Moon, S.-J.; Yum, J.-H.; Humphry-Baker, R.; Karlsson, K. M.; Hagberg, D. P.; Marinado, T.; Hagfeldt, A.; Sun, L.; Grätzel, M.; Nazeeruddin, M. K. *J. Phys. Chem. C* **2009**, *113*, 16816−16820.

(19) Chang, J. A.; Rhee, J. H.; Im, S. H.; Lee, Y. H.; Kim, H.-j.; Seok, S. I.; Nazeeruddin, M. K.; Grätzel, M. *Nano Lett.* **2010**, *10*, 2609−2612.

(20) Im, S. H.; Lim, C. −S.; Chang, J. A.; Lee, Y. H.; Maiti, N.; Kim, H. −j.; Nazeeruddin, Md. K.; Grätzel, M.; Seok, S. I. *Nano Lett.* **2011**, *11*, 4789−4793.

(21) Im, S. H.; Kim, H. −j.; Rhee, J. H.; Lim, C. −S.; Seok, S. I. *Energy Environ. Sci.* **2011**, *4*, 2799−2802.

(22) Cha, H.; Kong, H.; Chung, D. S.; Yun, W. M.; An, T. K.; Hwang, J.; Kim, Y.-H.; Shim, H.-K.; Park, C. E. *Org. Electron.* **2010**, *11*, 1534−1542.

(23) Shen, L.; Zhu, G.; Guo, W.; Tao, C.; Zhang, X.; Liu, C.; Chen, W.; Ruan, S.; Zhong, Z. *Appl. Phys. Lett.* **2008**, *92*, 073307−1−073307−3.

(24) Boix, P. P.; Lee, Y. H.; Fabregat-Santiago, F.; Im, S. H.; Mora-Sero, I.; Bisquert, J.; Seok, S. I. *ACS Nano* **2012**, *6*, 873−880.

(25) Masuda, K.; Ogawa, M.; Ohkita, H.; Benten, H.; Ito, S. *Sol. Energy Mater. Sol. Cells* **2009**, *93*, 762−767.